Proceedings of the 2010 IEEE
International Conference on Robotics and Biomimetics
December 14-18, 2010, Tianjin, China

Whisker-object contact speed affects radial distance estimation

Mat Evans[1], Charles W. Fox[1], Martin J. Pearson[2], Nathan F. Lepora[1] and Tony J. Prescott[1]

Abstract— **Whiskered mammals such as rats are experts in tactile perception. By actively palpating surfaces with their whiskers, rats and mice are capable of acute texture discrimination and shape perception. We present a novel system for investigating whisker-object contacts repeatably and reliably. Using an XY positioning robot and a biomimetic artificial whisker we can generate signals for different whisker-object contacts under a wide range of conditions. Our system is also capable of dynamically altering the velocity and direction of the contact based on sensory signals. This provides a means for investigating sensory motor interaction in the tactile domain. Here we implement active contact control, and investigate the effect that speed has on radial distance estimation when using different features for classification. In the case of a moving object contacting a whisker, magnitude of deflection can be ambiguous in distinguishing a nearby object moving slowly from a more distant object moving rapidly. This ambiguity can be resolved by finding robust features for contact speed, which then informs classification of radial distance. Our results are verified on a dataset from SCRATCHbot, a whiskered mobile robot. Building whiskered robots and modelling these tactile perception capabilities would allow exploration and navigation in environments where other sensory modalities are impaired, for example in dark, dusty or loud environments such as disaster areas.**

INTRODUCTION

To operate successfully in nocturnal or poorly-lit environments many animals have evolved non-visual sensory capacities, some of which have yet to be successfully replicated in robots. For instance, rodents, such as mice and rats, have evolved sophisticated tactile sensing systems based around their facial whiskers (known as vibrissae). Behavioural experiments have demonstrated that these animals can make judgements about the tactile properties of objects and surfaces with impressive accuracy. For instance, rats can extract the identity of a 30μm grating texture, in the dark, based on just one to three touches per whisker [4]; can display accurate judgments of a texture within 100 ms of initial whisker contact [3]; and can accurately determine object location in the whisker field [22][13]. Similarly, the Etruscan shrew - the smallest living mammal - can recognise and localise prey animals (insects) from a small number of fleeting whisker contacts, sufficient to allow fast and precisely targeted attacks [1]. Processing can also be very fast. For instance in the mouse, whisker contact signals can reach the barrel cortex – from where they can begin to affect processing in behaviour-related areas such as the motor cortex, the superior colliculus, and cerebellum – in just 7 milliseconds [9]. Robots with tactile sensing capabilities approaching those of rodents would excel in environments where many other sensory modalities are impaired. In dusty, smoky or loud environments such as disaster areas and war zones where sensory systems operating in the modalities of sight and sound may be compromised. Whiskers themselves are inexpensive, mechanically simple elements. Whiskers have no sensory elements along their length, deflections are processed by sensors at the base, making them relatively robust to damage. In contrast, an artificial hand will have sensor elements at or near the tips of its digits where they will be much more vulnerable to wear and tear. Together these features make whisker based tactile sensors ideal for mobile robotics.

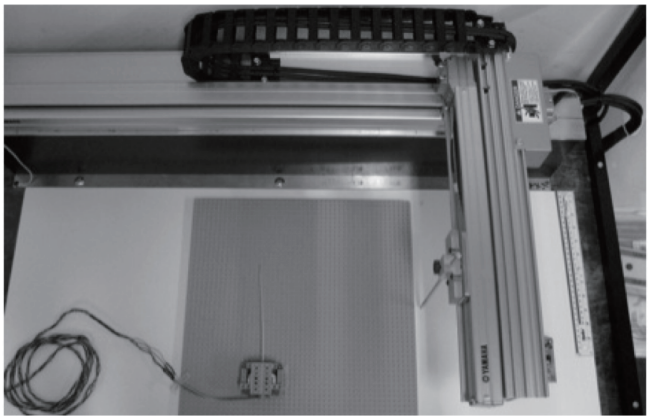

Fig. 1. The XY positioning robot. The whisker was deflected by the robot along the X axis through movements in a clockwise or anticlockwise direction as viewed from above.

Recent years have seen many whiskered robots being developed (for example, SCRATCHbot [17] [12]), addressing numerous aspects of tactile perception (see [19] for a recent review). Previous work has shown that information about texture, distance to contact, and shape can be extracted from signals obtained when an artificial whisker is moved against a surface [10][6][14][8].

The XY positioning robot. Developing more sophisticated models of whisker-based perception has been problematic. In modalities such as vision and audition it is generally quite easy to present stimuli to a passive sensor on a robot, or images and tones can be simulated and used to train a computational model. There is no obvious analog for tactile stimuli, and the true nature of whisker-object interactions is too poorly understood to be simulated accurately. Whiskers are especially difficult to simulate, as they have very low mass but high spring constants when

[1] Active Touch Laboratory, Department of Psychology, University of Sheffield, Western Bank, Sheffield. S10 2TN, UK. *mat.evans@shef.ac.uk*
[2] Bristol Robotics Laboratory, Du Pont Building, Bristol Business Park, Coldharbour Lane, Frenchay, Bristol. BS16 1QD, UK

978-1-4244-9318-0/10/$26.00 © 2010 IEEE

modelled as a series of masses on rotational springs, leading to numerical instabilities. Additionally when the parameters of a whisker-object contact become more numerous (e.g. speed and radial distance to contact, surface texture, orientation and softness etc) it becomes very difficult to constrain the contact and generate reliable signals in either simulated or physical robots. For these reasons acquiring sufficient examples of carefully controlled whisker contacts with tactile stimuli to train models and classifiers has proved difficult. We present a novel system for generating large, repeatable, sets of deflection signals from whisker-object contacts. An XY positioning robot is programmed to move objects into an artificial whisker sensor Fig.1. Deflections for the whisker are streamed to a PC, and can be processed in real time to control subsequent robot movement.

Under passive deflections an object moved by the robot arm makes contact with the artificial whisker and deflects the whisker through a large angle. When deflection reaches a critical point the whisker loses friction with the object, deforms and deflects past the object and goes through oscillatory ringing until the energy dissipates and the whisker comes to rest.

However, in addition to passive touch experiments we are also able to use our experimental setup to investigate active sensing. In this case we mimic a control policy that we have observed in rats in our own laboratory whereby the protraction of a whisker ceases rapidly on contact with a surface and whisker then begins to retract [16]. In contrast to the passive case, this policy, which we call Minimal Impingement (MI), keeps the amplitude and duration of whisker deflection within a limited range, and also keeps whisker ringing after contact to a minimum. An additional benefit is that the forces acting on the whisker are much smaller, meaning whisker breakage is less likely – an important consideration for autonomous robotics.

Having established our motivation and methodological direction, the remainder of this paper describes our initial experiments exploring the space of whisker-object contacts, and the feature based classifiers we have developed to reliably encode this space. The classifiers are then verified on a preliminary data set from the SCRATCHbot whiskered robot [17].

METHODS

An XY positioning robot (Yamaha-PXYX, Yamaha Robotics) (see Fig.1) was used to move objects into the whisker. The robot has a movement range of 350×650mm, and can move up to 720mm/s. Repeatability of the robot is ±0.01mm, and the maximum load it can carry is 1.5kg. Objects are carried by the robot into an artificial whisker fixed to the table, as this allows us to control the contact as carefully as possible. Moving the whisker into an object would cause the whisker to oscillate unpredictably during movement between contacts, and as a result each contact would be slightly different. A controller (Yamaha RCX 222, 2-axis robot controller) takes instructions from a PC through an RS232 cable, and the controller interprets the instructions, completes path integration, and drives the motors. Instructions for the robot are generated inside a MATLAB (www.mathworks.com) loop, and can be easily updated during robot operation, for example to react to whisker input.

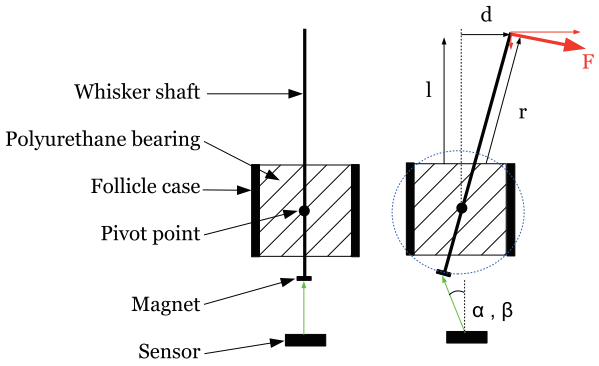

Fig. 2. Diagram of the artificial whisker Hall effect sensor.

The Whisker. A whisker sensor was taken from the SCRATCHbot robot platform [17][19]. Technical details of the whisker can be found in [6]. A tapered, flexible plastic whisker shaft, ≈5 times scale models of a rat whisker (185mm long, linearly tapered from a diameter of 0.5mm at the tip to 3mm at the base), was mounted into an inflexible rubber-filled tube, or 'follicle' case. A tri-axis Hall effect sensor (Melexis MLX90333 [15]) mounted in the follicle case measures the deflection of a magnet fixed to the base of the whisker shaft Fig.2. The Hall effect sensor IC was programmed to generate two voltages, the magnitudes of which being proportional to the two orthogonal displacement angles (α, β) of the magnet from its resting position above the sensor (see Fig. 2). As forces are applied to the whisker shaft, the moment experienced at the base will rotate the magnet around the pivot point, nominally in the centre of the polyurethane bearing. A trigonometric operation in the DSP core of the Hall sensor IC decouples the alpha and beta angles and removes the z-component introduced by the arc of travel of the magnet, as indicated by the blue dotted line in Fig. 2. This operation ensures that the output voltages from the IC are linearly proportional to the tangent component of the alpha and beta angles, or x and y as they will be referred to hereafter.

Data. Deflections of the whisker were transmitted through the hall effect sensors to a LabJack UE9 USB data acquisition card (www.labjack.com) at a rate of 1 kHz for each of the x and y directions. Each trial lasted 4s. This data was sent to a computer through the BRAHMS middle-ware (brahms.sourceforge.net) for analysis in MATLAB.

Robot control. Minimal impingement was implemented by instructing the robot to move an object into the whisker at a given speed until a deflection threshold is crossed, at which point the robot retracts the object as fast as possible (720mm/s). Temporal latency for the loop is ≈ 300ms from initial contact due to the controller duty cycle.

The task. Preliminary investigations highlighted that the

closest contact that could be made by the whisker at without saturating the Hall effect sensor very quickly was ≈80mm from the base. Contacts at less than 5mm from the tip did not deflect the base of the whisker for long enough before slipping past to allow an MI type contact. Therefore, the 185mm length whiskers provide a 100mm range of radial distances. Contact speeds above 216mm/s either cause the whisker to slip past the object before a retraction, or saturates the sensors. 36mm/s was the lower bound on the speed for practical reasons. Contacts were sampled at radial distance intervals of 1mm, and speed intervals of ≈7mm/s over the previously described ranges. In total 101 radial distances and 26 speeds were sampled, giving 2626 different radial distance and speed combinations. Contact combinations were randomly interleaved to limit any affects of whisker properties changing over time. For each contact combination the whisker was deflected by the robot in both a clockwise and anticlockwise directions (-ve and +ve in x, see Fig.1), ensuring that the whisker did not bend over time through repeated unilateral deflections. The experiment was performed twice to generate sufficient data for classification. Data from each trial was stored separately. Deflections from the clockwise robot movement trials (-ve in x) were converted so all data samples were equivalent. Trials were ordered into arrays by speed and radial distance to contact. Each trial was aligned to peak deflection, and shortened to only the 325ms either side of the peak deflection.

Speed of contact confounds radial distance detection. The object properties we chose to manipulate and recognise were radial distance to contact from the base, and contact speed. The task is to recognise these two parameters *simultaneously* under varying conditions.

Previous work [11][24] has shown that a rat could encode the radial distance to contact along a whisker by monitoring the magnitude of forces (or moments) at the base. Others have suggested that the increased firing rate of cells in the whisker sensory nerve, for contacts close to the base, could be due to the increased moments at the whisker base, indicating that this moment information is available to the rat [22]. In controlled experiments it has been shown that a rat can discriminate apertures of different widths, down to a difference of ≈3mm [13]. When modelled as a cylindrical elastic beam, the relationship between radial distance to contact r, moment (or torque) at the base M and whisker deflection angle θ can be expressed [11] as;

$$r = 3EI_{\text{base}}\frac{\theta}{M}, \tag{1}$$

where E is the elastic modulus, and I_{base} is the area moment of inertia at the base of the whisker. In this equation the interaction of deflection angle θ and M gives you a value for radial distance to contact. However, the equation would need to be modified to account for situations where contact speed is a variable.

Static beam equations, and analyses relying on instantaneous measures of moments only account for the dynamic properties of objects if two observations are made. If an object collides with a whisker at the same location but at different speeds it will induce different forces at the base. For example, under the right conditions the moment at the base will be the same for a slowly moving object contacting near the base, and a quick object near the tip (see Fig.3 for a demonstration of this).

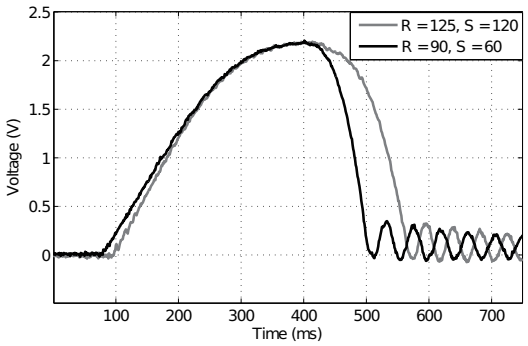

Fig. 3. Example deflection signals from the artificial whisker. Magnitude of deflection, or force, has been used as a discriminator of radial distance to contact. Here the two traces are at different radial distances, but create the same magnitude of deflection.

This ambiguity in the signal cannot be accounted for with a single observation, an additional observation, or invariant feature in the signal, must be found in order to discriminate these two properties of the collision. For example by taking rate of change of moment and θ, or by taking the longitudinal force [21]

In the present study we find features in the data that correspond to radial distance to contact and object speed. Successful classification relies either on finding the contact speed before conducting a radial distance estimation, or discriminating two properties simultaneously (e.g. [7]).In the analysis we assess simple feature-based classifiers, and compare the performance of different features in isolation and combination.

RESULTS

The data were separated into training and test sets that were each 2 complete data sets of 26 speeds and 101 radial distances. Signals were placed in the training or test sets at random from the original data. For each feature, classifiers were developed on the training sets, and performance was determined on the test set.

Feature based classifiers. Inspection of the data showed that peak deflection magnitude could be used as a feature for radial distance discrimination at a given speed. Deflection magnitude was taken as the Hall effect sensor output voltage at peak deflection, which is proportional to the bending moment. Feature f_1 can be defined as,

$$f_1 = \max_t \theta(t), \tag{2}$$

where $\theta(t)$ is the deflection magnitude varying with time, measured by the Hall effect sensor in volts. Note that $t(f_1) = t(\max_t \theta(t))$

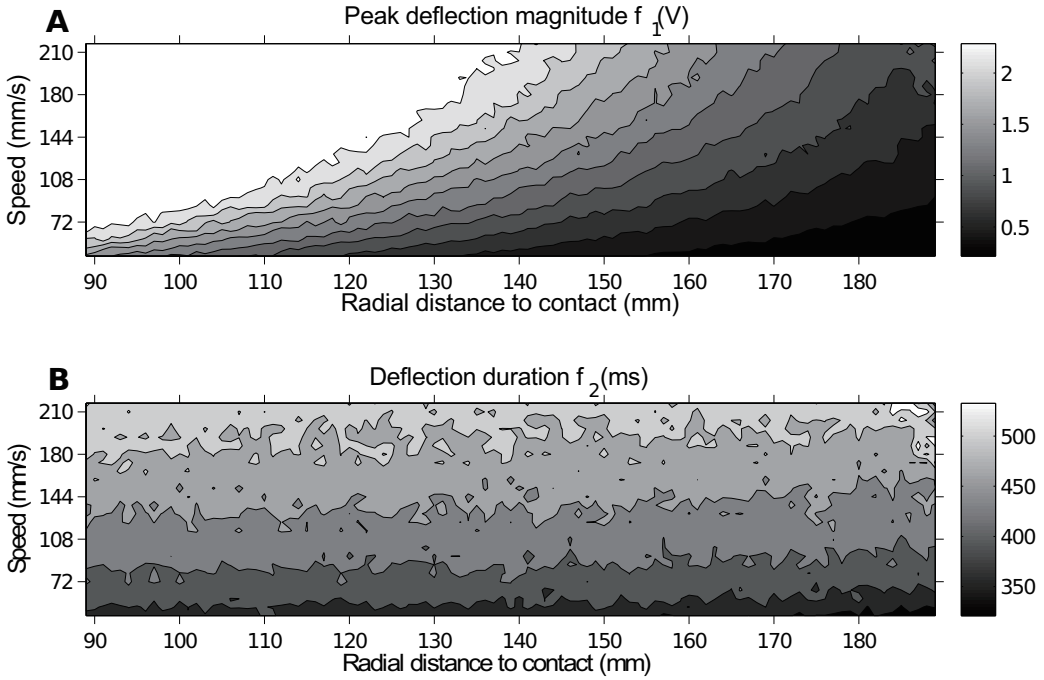

Fig. 4. A contour plot of peak deflection magnitude and duration for each contact. Each point in the image corresponds to a location in the speed-radial distance space which is equivalent in both plots. (a) Peak deflection magnitude f_1, brightness indicates higher deflection magnitude, measured in volts. (b) Deflection duration f_2, brightness indicates greater duration (measured in ms).

Similarly, contact speed could be discriminated using deflection duration. Deflection duration was taken as the width of the deflection peak (prominent initial deflection in each trace of Fig.3). Deflection duration was measured using a threshold crossing on the sensor output. When Hall effect sensor output exceeded 0.05V a timer was initiated (t_1), and when Hall output subsequently fell below this threshold the timer was stopped (t_2). Feature f_2 can be defined as,

$$t_1 = \min\{\mathrm{t} : \theta(\mathrm{t}) \geq \gamma\}, \tag{3}$$

$$t_2 = \min\{\mathrm{t} : \theta(\mathrm{t}) \leq \gamma, \mathrm{t}_2 > \mathrm{t}_1\}, \tag{4}$$

$$f_2 = t_2 - t_1, \tag{5}$$

where γ is the threshold and f_2 was measured in ms. Fig.4 shows the object-contact space for f_1 and f_2 in graphical format.

As an additional feature peak rate of change of deflection $\dot{\theta}(t)$ was used. Rate of change of moment $\dot{M}$ and deflection angle $\dot{\theta}$ have each been proposed as biologically plausible alternatives to the absolute values used in elastic beam equations for radial distance detection (Eq. 1) [2] [20]. Since the output of the Hall effect sensor corresponds to deflection magnitude, which is in itself proportional to the bending moment, we found a proxy for rate of change of moment by computing the rate of change of deflection of the whisker, $\dot{\theta}(t)$. To generate $\dot{\theta}$ each input signal was down-sampled to 100Hz, a derivative was taken and the peak derivative from the protraction period of each trial was taken as $\dot{\theta}(t)$. Feature f_3 can be defined as,

$$f_3 = \max_{\mathrm{t}} \dot{\theta}(\mathrm{t}), \tag{6}$$

for each trial the peak $\dot{\theta}$ was taken during the initial deflection of the whisker, $t < t(f_1)$, where $t(f_1)$ is the time at which the f_1 occurs.

A model was generated of the relationship between each feature and the corresponding contact property by fitting a cubic polynomial to the training data in MATLAB, for example to find an estimate of radial distance $\hat{r}$,

$$\hat{r} = a_3 f_1^3 + a_2 f_1^2 + a_1 f_1 + a_0, \tag{7}$$

was fitted to the data with a linear-in-the-parameters regression on the cubic, to find (a_0, a_1, a_2, a_3) by least squares.

In the case of simultaneous radius and speed classification, speed is classified first with f_2, then radial distance is classified with a model fitted to a smaller region of the f_1 or f_3 space.

Classification performance. Fig. 4 shows features f_1 and f_2 for each radius and speed combination. Looking at both plots at the same time shows the interaction of deflection magnitude and duration across the feature spaces. Alone, deflection magnitude f_1 is an ambiguous predictor for radial distance Fig. 4(a). By using deflection duration f_2 as a measure of speed Fig. 4(b), it is possible to limit the region of Fig. 4(a) over which to perform the radial distance discrimination, thus improving classification. The results of the classification are summarised in Table I.

Single feature classification. When used alone, peak deflection magnitude f_1 allows discrimination of 46% of inputs

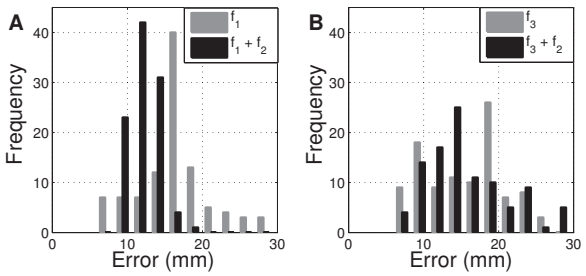

Fig. 5. Histograms of the mean error for radial distance classification in each condition. Combining each classifier with a discriminator for speed improved classification, both by decreasing the mean (moving the histogram peak towards zero) and by reducing variance (width of the histogram).

to within 10mm over the 101mm range. Mean error was 13.6 mm. Deflection duration f_2 was capable of classifying 98% of inputs to within 70mm/s for speed, over the 216mm/s range. Mean error here was 20mm/s. Classification of radial distance based on rate of change of deflection magnitude f_3 was successful in 50% of inputs to within 10mm over the 101mm range. Mean error was 15.6mm.

Multi-feature classification. In each case combining classifiers improved radial distance detection. Combining deflection duration f_2 and peak deflection magnitude f_1 results in improved radial distance classification of 74% to within 10mm. Mean error was reduced to 8.4mm.

Combining deflection duration f_2 classification with rate of change of deflection f_3 again results in improved radial distance classification of 54% to within 10mm. Mean error was reduced to 11.4mm.

Histograms of mean errors for classification are shown in Fig.5.

TABLE I

MEAN CLASSIFICATION PERFORMANCE FOR EACH CONDITION OVER DIFFERENT VERIFICATION WINDOWS.

% Correct	f_1	f_1+f_2	f_3	f_3+f_2
$\leq$ 5mm	23.6%	45.2%	28.1%	36.0%
$\leq$ 10mm	46.1%	74.4%	50.0%	54.4%
$\leq$ 15mm	46.2%	74.5%	50.1%	54.5%

Verification on SCRATCHbot data. A small dataset was collected on the SCRATCHbot whiskered robot platform [18][17]. The robot was kept stationary while it whisked into a vertical pole at 3 different radial distances (70, 100 and 130mm), and 3 whisk speeds (2, 4 and 6Hz). This dataset is too small to do an analysis similar to that conducted on the XY table data, but some useful insights can be gained from it. SCRATCHbot data was inspected to see whether the same features found in the XY table generated signals would be present in a less well constrained situation (see Fig. 7). A key difference between data from SCRATCHbot and that from the XY table is the way whisker speed affects contact duration. Since SCRATCHbot is performing active whisking, increased whisk speed results in a shorter contact duration. However, though the direction of the relationship is reversed, whisk speed still predictably affects contact duration. As

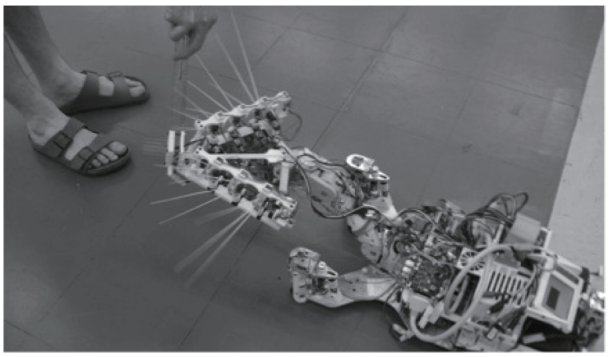

Fig. 6. The SCRATCHbot whiskered mobile robot. To collect data for this experiment the robot platform was kept stationary while it whisked into a pole at varying radial distances to contact, and whisk speed.

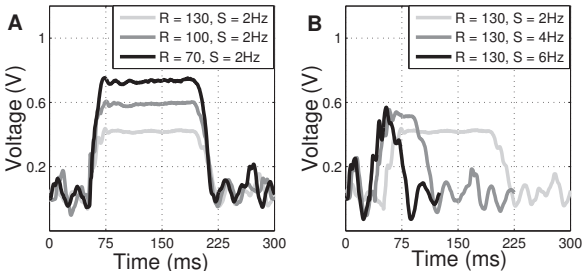

Fig. 7. Properties of the deflections match closely to those from the XY table. (a) 3 deflections at different radial distances (R, in mm), but the same speed (S, in Hz). Peak deflection height varies predictably with radial distance. (b) 3 deflections at the same radial distance but at different speeds. Contact duration varies predictably with speed.

in the XY table data, whisking at the same radial distance but different speeds affects peak deflection magnitude (as can be seen in Fig. 7(b)). On SCRATCHbot, as on the XY table, accurate radial distance estimation must involve taking whisker contact speed into account.

DISCUSSION AND CONCLUDING REMARKS

The results presented here compare favourably with the sensory capabilities of rats. Rats have been shown to be capable of discriminating apertures differing in width by 5mm, corresponding to a radial distance difference of 2.5mm per whisker [13]. Since the longest rat whiskers are 50–60mm in length, a 2.5mm discrimination corresponds to an acuity of ≈4–5% of whisker length. A discrimination acuity of 8.4mm on an 185mm whisker corresponds to an acuity 4.5% of whisker length.

It is important to consider that a rat has ≈30 whiskers on each side of its head. Combining information from multiple whiskers may improve the reliability of classification, for example by providing a means to remove independent noise from the signal. This is an approach we hope to investigate in the future. Rate of change of moment has been proposed [2] as a biologically plausible method of measuring radial distance to contact, as biological systems are poor at measuring absolute values. Though performance of a classifier using $\dot{\theta}$ information is poorer than that of a classifier using absolute

values, it is still well above chance (chance performance = 20% success to within 10 mm). Classifier performance is improved when combined with an additional speed of contact feature, f_2.

When trying to discern a whisker contact property, such as radial distance to contact, any observation that a classification can be based on will always be affected by the nature of the contact. In the rat whisker system, contacts are adaptively controlled [16]. Though the true purpose of this control is not entirely understood, it is clear that whisker contact speed and force has a large impact on the signals that are produced at the base. We have shown previously that whisker contact speed, and object location have an effect on whisker based texture discrimination [10][6], and that interacting with a surface within certain ranges of speed and at particular regions of the whisker may indicate a 'sweet spot' of whisker object interaction [7]. The rat may be adaptively controlling whisker movement to constrain the ambiguity in the vibrissa deflection signals.

Though in artificial whiskers deflection signals are ambiguous under certain conditions, it is possible to discern certain contact properties from robust features. Subsequent classification can be improved when these contact features are taken into account. Data from the SCRATCHbot robot platform shows that the features found in analysis of XY table data still apply. Going forward we hope to test these classifiers more thoroughly on SCRATCHbot in task based situations. Robust reports of local object features can then be used as inputs to a system of tactile SLAM [5][23].

Steps have been made to explore whisker-object contact space, and in future we hope to utilise the XY table system presently described to investigate further object properties. Knowing contact speed allows better radial distance estimation, which in turn can be used for the discrimination of corners and surface curvature [20]. Discerning the orientation and location of a surface is critical to the discrimination of texture [10]. It is clear that whisker based tactile perception is critically dependent on properties of whisker-object contact. In autonomous robotics, reciprocal sensory motor interaction of this sort can be used to maximise the sensitivity and reliability of a system. Simultaneous speed and radial distance detection is a step towards this goal.

Acknowledgements This work supported by the EPSRC Doctoral Training Scheme and EU grants ICEA (IST-027819) and BIOTACT (ICT-215910).

REFERENCES

[1] Farzana Anjum, Hendrik Turni, Paul G H Mulder, Johannes van der Burg, and Michael Brecht. Tactile guidance of prey capture in etruscan shrews. *Proc Natl Acad Sci U S A*, 103(44):16544–16549, 2006.

[2] J Alexander Birdwell, Joseph H Solomon, Montakan Thajchayapong, Michael A Taylor, Matthew Cheely, R Blythe Towal, Jorg Conradt, and Mitra J Z Hartmann. Biomechanical models for radial distance determination by the rat vibrissal system. *J Neurophysiol*, 98(4):2439–2455, 2007.

[3] George E. Carvell and Daniel J. Simons. Biometric analyses of vibrissal tactile discrimination in the rat. *J Neurosci*, 10(8):2638–2648, 1990.

[4] Mathew E Diamond, Moritz von Heimendahl, Per Magne Knutsen, David Kleinfeld, and Ehud Ahissar. 'where' and 'what' in the whisker sensorimotor system. *Nat Rev Neurosci*, 9(8):601–612, 2008 Aug.

[5] Gamini. Dissanayake, Paul. Newman, Steven. Clark, Hugh. Durrant-Whyte, and M. Csorba. A solution to the simultaneous localization and map building (slam) problem. *IEEE Transactions on Robotics and Automation*, 17(3):229–241, 2001.

[6] Mat Evans, Charles W Fox, Martin J. Pearson, and Tony J Prescott. Spectral template based classification of robotic whisker sensor signals in a floor texture discrimination task. In T Kyriacou, U. Nehmzow, C. Melhuish, and M. Witkowski, editors, *Proceedings of Towards Autonomous Robotic Systems (TAROS 2009)*, pages 19–24, 2009.

[7] Mat. Evans, Charles W. Fox, Martin J. Pearson, and Tony J Prescott. Tactile discrimination using template classifiers: Towards a model of feature extraction in mammalian vibrissal systems. In *Proceedings of the 11th International Conference on Simulation of Adaptive Behaviour*, 2010.

[8] Miriam. Fend, Simon. Bovet, Hiroshi. Yokoi, and Rolf. Pfeifer. An active artificial whisker array for texture discrimination. In *2003 IEEE/RSJ International Conference on Intelligent Robots and Systems, 2003.(IROS 2003). Proceedings*, volume 2, 2003.

[9] Isabelle Ferezou, Sonia Bolea, and Carl C H Petersen. Visualizing the cortical representation of whisker touch: voltage-sensitive dye imaging in freely moving mice. *Neuron*, 50(4):617–629, 2006.

[10] Charles W Fox, Ben Mitchinson, Martin J Pearson, Anthony G Pipe, and Tony J Prescott. Contact type dependency of texture classification in a whiskered mobile robot. *Autonomous Robots*, 2009.

[11] Venkatesh Gopal and Mitra J Z Hartmann. Using hardware models to quantify sensory data acquisition across the rat vibrissal array. *Bioinspir Biomim*, 2(4):S135–45, 2007.

[12] DaeEun Kim and Ralf Moller. Biomimetic whiskers for shape recognition. *Robotics and Autonomous Systems*, 55:229–243, 2007.

[13] David J Krupa, Matthew S Matell, Amy J Brisben, Laura M Oliveira, and Miguel A Nicolelis. Behavioral properties of the trigeminal somatosensory system in rats performing whisker-dependent tactile discriminations. *J Neurosci*, 21(15):5752–5763, 2001.

[14] Nathan.F Lepora, Mat Evans, Charles. W. Fox, Kevin Gurney, and Tony.J Prescott. Naive bayes texture classification applied to whisker data from a moving robot. In *Proceedings of the 2010 international joint conference on Neural Networks*, pages 2970 – 2877, 2010.

[15] Melexis. www.melexis.com/assets/mlx90333_datasheet_5276.aspx.

[16] Ben Mitchinson, Chris J Martin, Robyn A Grant, and Tony J Prescott. Feedback control in active sensing: rat exploratory whisking is modulated by environmental contact. *Proc Biol Sci*, 274(1613):1035–1041, 2007.

[17] Martin J. Pearson, Ben Mitchinson, Jason Welsby, Tony G Pipe, and Tony J. Prescott. Scratchbot: Active tactile sensing in a whiskered mobile robot. In *Proceedings of the 11th International Conference on Simulation of Adaptive Behaviour (SAB).*, 2010.

[18] Tony J. Prescott, Martin J. Pearson, Charles W. Fox, Mat. Evans, Ben Mitchinson, Sean Anderson, and Anthony G Pipe. Towards biomimetic vibrissal tactile sensing for robot exploration, navigation, and object recognition in hazardous environments. In *In Proceedings of 4th IARP workshop: Robots for risky Interventions and Environmental Surveillance- maintenance (RISE)*, 2010.

[19] Tony J Prescott, Martin J. Pearson, Ben Mitchinson, J Charles W. Sullivan, and Anthony G. Pipe. Whisking with robots from rat vibrissae to biomimetic technology for active touch. *IEEE Robotics and Automation Magazine*, 16(3):42–50, 2009.

[20] Joseph H. Solomon and Mitra J Hartmann. Extracting object contours with the sweep of a robotic whisker using torque information. *The International Journal of Robotics Research*, 2009.

[21] Maik C. Stüttgen, Stephanie Kullmann, and Cornelius Schwarz. Responses of rat trigeminal ganglion neurons to longitudinal whisker stimulation. *J Neurophysiol*, 100:1879–1884, August 2008.

[22] Marcin Szwed, Knarik Bagdasarian, Barak Blumenfeld, Omri Barak, Dori Derdikman, and Ehud Ahissar. Responses of trigeminal ganglion neurons to the radial distance of contact during active vibrissal touch. *J Neurophysiol*, 95(2):791–802, 2006.

[23] Sebastian Thrun. Probabilistic robotics. *Communications of the ACM*, 45(3):52–57, March 2002.

[24] Naohiro. Ueno, Mikhail.M. Svinin, and Makoto. Kaneko. Dynamic contact sensing by flexible beam. *Mechatronics, IEEE/ASME Transactions on*, 3(4):254–264, Dec 1998.